J. Chem. Lett. 3 (2022) 169-173

Research Article

Journal of Chemistry Letters
journal homepage: www.jchemlett.com
ISSN (online):2717-1892

Venlafaxine Interaction with Fullerene (C_{20}): DFT Studies

Mohammad Reza Jalali Sarvestani

Young Researchers and Elite Club, Yadegar-e-Imam Khomeini (RAH) Shahr-e-Rey Branch, Islamic Azad University, Tehran, Iran
Corresponding author email address: Rezajalali93@yahoo.com

ARTICLE INFO

Article history:
Received 1 October 2022
Received in revised form 20 November 2022
Accepted 10 December 2022
Available online 20 December 2022

Keywords:
Venlafaxine
Fullerene (C_{20})
Adsorption
Density functional theory

ABSTRACT

Rapid and accurate determination of venlafaxine (VNF) as an antidepressant medicine is of great importance. Therefore, in this research, (VNF) adsorption on the surface of fullerene C_{20} was studied by density functional theory computations. The calculated adsorption energies showed VNF interaction with C_{20} is experimentally possible. The negative values of enthalpy alterations, Gibbs free energy changes and great values of thermodynamic constants indicated the adsorption process is spontaneous. The negative values of adsorption enthalpy changes revealed the interaction of VNF with fullerene is exothermic. The bandgap of fullerene after adsorption of VNF increased %296.923 from 1.950 (eV) to 7.740 (eV) indicating the electrical conductivity of fullerene experienced a very sharp alteration during the interaction process. Therefore, C_{20} can be used as a sensor for electrochemical detection of VNF. The influence of the temperature on the VNF interaction with fullerene was also investigated and the results showed the adsorption process is more favorable in the lower temperatures.

Introduction

Venlafaxine (VNF, Figure 1), is an antidepressant medicine that is prescribed for the treatment of depression, eating disorders, neuropathic pains and migraine prevention [1-3]. NTP is one of the best-selling antidepressants that induces its therapeutic effects by inhibiting the uptake of norepinephrine, serotonin and dopamine [4-6]. However, in high doses, VNF can be highly toxic and its adverse effects are agitation, drowsiness, coma, seizures and serotonin syndrome. In this respect, VNF determination is very important. To date, various analytical techniques such as high-performance liquid chromatography (HPLC), gas chromatography (GC), fluorimetry, capillary electrophoresis and UV-Visible spectrophotometry have been reported for the quantitation of VNF [7-9].

However, these methods are too expensive, time-consuming and tedious. Besides, large amounts of organic solvents are used in the mentioned methods. But, electrochemical and thermal sensors are prominent alternatives for the refereed analytical techniques because these types of sensors are rapid, simple, economic, portable, selective and sensitive devices that can determine the amount of the analyte with excellent accuracy and repeatability [10-14]. However, the first step in the development of a new electrochemical and thermal sensor is to find a recognition element that interacts with the analyte selectively and this interaction should lead to a considerable change in the electrochemical and thermal conductivity of the utilized recognition element which is used as a signal for determination of the analyte concentration [15-17].

On the other hand, fullerene (C_{20}, Figure 1b) is the smallest nanomaterial with a dodecahedral cage structure [18]. The structure of this fullerene is highly curved and it is composed of pentagonal rings. C_{20} has unique traits that make it an eminent sensing material like high conductance, great surface area/ volume ratio and excellent reactivity [19]. In this respect, the goal of this study is to evaluate the sensing performance of C_{20} for thermal and electrochemical detection of NTP by density functional theory simulations.

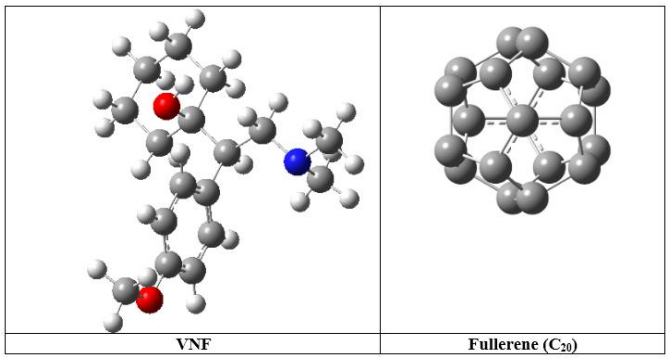

Figure 1. the chemical structure of VNF and C_{20}

Results and Discussion

In order to find the most stable configuration, the adsorption process was investigated at two different positions. As can be seen from the presented optimized structures of VNF-fullerene complexes at Figure 2, in A-Conformer, the nanostructure is inserted near the benzene ring and amine group of VNF and in the B-Conformer, fullerene is placed near the cyclohexanol group of VNF. The calculated total electronic energies in table 1, showed that A-Conformer is more energetically stable than B-Conformer. Besides, the computed adsorption energies indicated VNF interaction with the adsorbent is experimentally feasible and the adsorption process is more favorable at B-conformer. In order to obtain more information about the adsorption mechanism, the NBO computations were also carried out and the results showed no chemical bonds have been created between fullerene and VNF and the studied interaction is a physisorption [9-11].

The maximum (ν_{max}) and lowest vibrational frequencies (ν_{min}) of structures were also calculated by IR computations. As can be seen from Table 1, no negative frequency was observed for the studied structures. Therefore, all of the investigated structures are in a true local minimum [12].

The dipole moments of the structures were also computed. As the provided data at table 1 reveals clearly when VNF adsorbs on the surface of fullerene the dipole moment increases from 2.480 to 8.450 and 10.590 at A and B conformers respectively. Therefore, the solubility and bioavailability of VNF enhance significantly when it is adsorbed on the surface of fullerene [13].

Table 1. The structural parameters of VNF, C_{20} and their complexes

	Total electronic energy (a.u)	**Adsorption energy (kJ/mol)**	**ZPE (kJ/mol)**	**ν_{min} (cm^{-1})**	**ν_{max} (cm^{-1})**	**Dipole Moment (Debye)**
VNF	-853.102	---	1298.120	21.785	4235.607	2.480
C_{20}	-747.196	---	325.260	261.392	1690.640	0.000
A-Conformer	-1600.308	-23.994	1645.870	1.959	4235.666	8.450
B-Conformer	-1600.324	-67.019	1648.130	12.372	4296.857	10.590

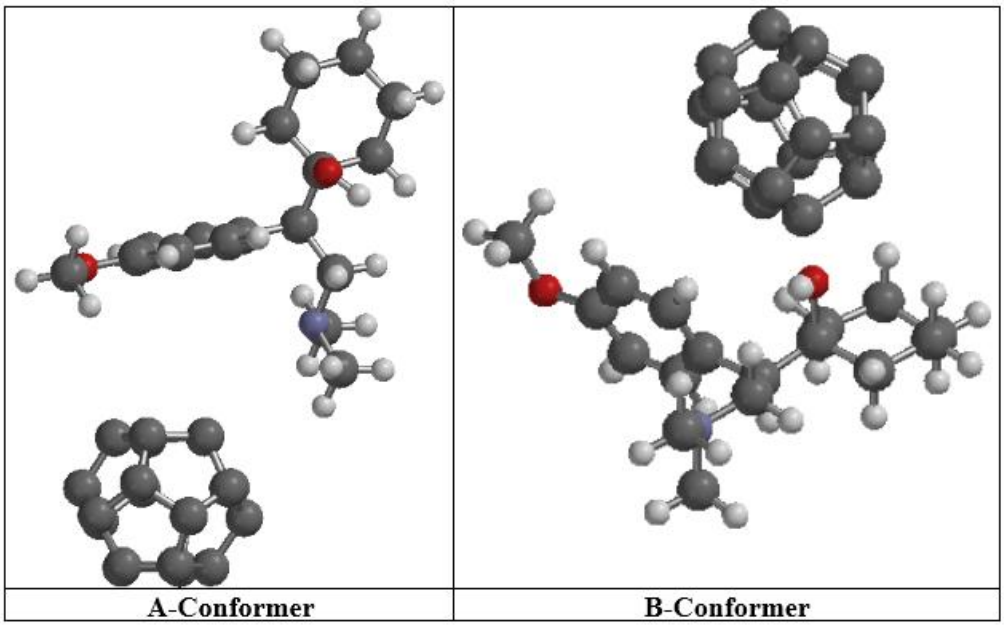

Figure 2. Optimized structures of VNF-C_{20} complexes

The thermodynamic parameters of VNF adsorption process were also calculated and the results are presented in Figure 3. As can be seen, the adsorption Gibbs free energy (ΔG_{ad}) is negative at both conformers which indicates the interaction process is spontaneous. The values thermodynamic equilibrium constants (K_{th}) are positive and little for both conformers that indicates the interaction is reversible and equilibrium. The impact of

temperature on both parameters was also checked out and the results demonstrates the interaction process is more favorable at lower temperatures [14].

The positive values of adsorption entropy changes (Δs_{ad}) showed the adsorption process is also appropriate in terms of entropy and the chaos has increased when VNF adosrbs on the surface of fullerene [15].

The negative values of adsorption enthalpy changes (ΔH_{ad}) showed the interaction process is exothermic [16]. Frontier molecular orbital (FMO) parameters including bandgap (Eg), chemical hardness (η), chemical potential (μ), electrophilicity (ω) and maximum transferred charge (ΔN_{max}) were also calculated and the results are given in Table 2. As can be seen, the bandgap value of fullerene increased significantly after VNF interaction from 1.950 (ev) to 7.740 (ev) and 5.393 for A and B conformers respectively, indicating the sharp alteration of electrical conductivity during the adsorption procedure. There, fullerene is an appropriate electrocatalytic sensing material for the development of new electrochemical sensors for the determination of VNF. The chemical hardness of VNF decline from 6.185 (eV) to 3.870 (eV) and 2.697 (eV) after interaction with fullerene indicating VNF-Fullerene complexes are more chemically reactive. The negative values of chemical potential for all of the structures showed all of the investigated structures are thermodynamically stable. The increasing of electrophilicity and maximum transferred charge of NTP after adsorption on the fullerene surface showed VNF-fullerene complexes are more electrophile than pure VNF without nanostructure.

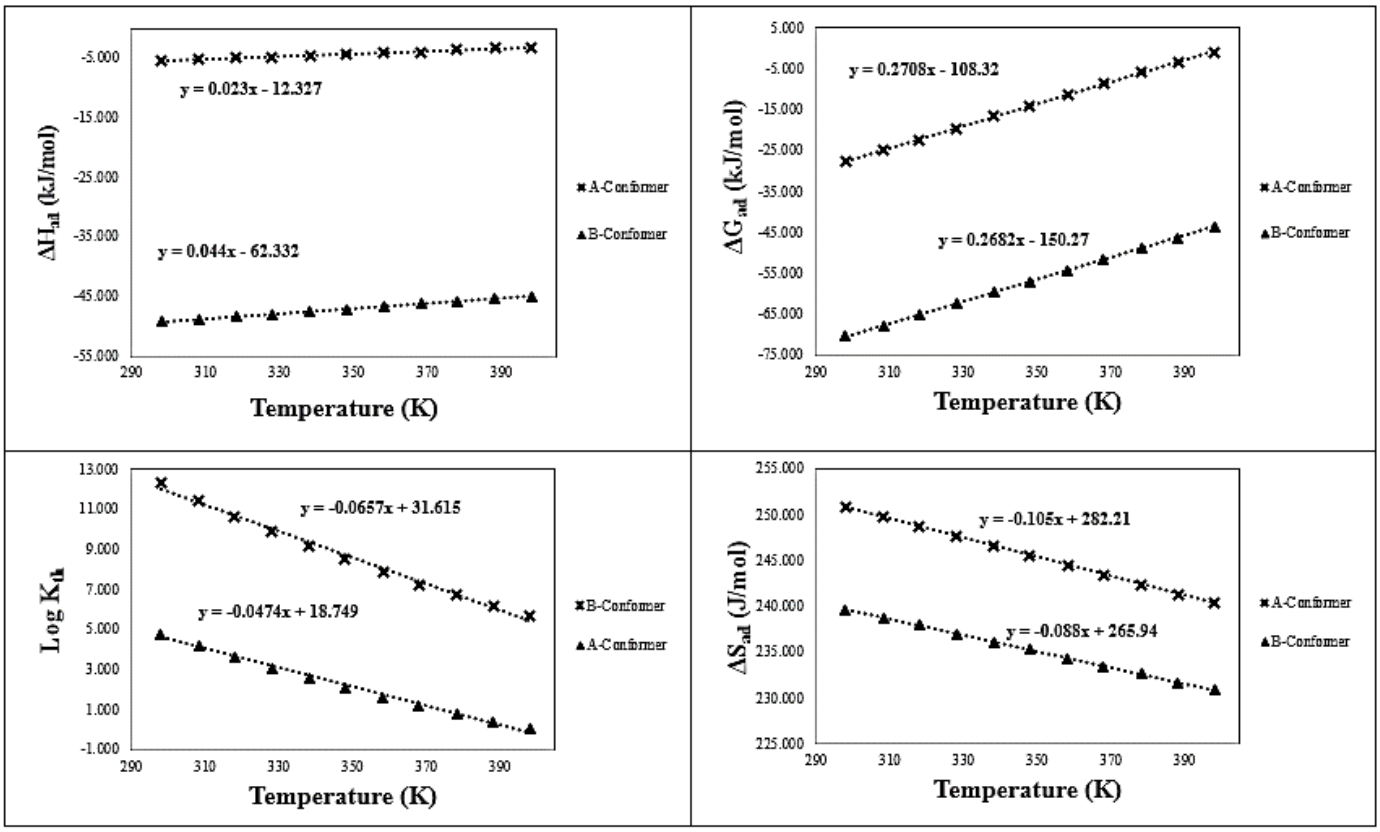

Figure 3. the values of ΔH_{ad} , ΔG_{ad}, the logatim of K_{th} and ΔS_{ad} as a function of temperature in the range of 298-398 K.

Table 2. The FMO parameters of NTP, C_{20} and their complexes

NO	E_{HOMO} (eV)	E_{LUMO} (eV)	Eg (eV)	%ΔEg	η (eV)	μ (eV)	ω (eV)	ΔN_{max} (eV)
VNF	-6.240	6.130	12.370	---	6.185	-0.055	0.000	0.009
C_{20}	-5.060	-3.110	1.950	---	0.975	-4.085	8.558	4.190
A-Conformer	-4.440	3.300	7.740	296.923	3.870	-0.570	0.042	0.147
B-Conformer	-3.280	2.113	5.393	176.564	2.697	-0.584	0.063	0.216

Computational Details

The structures of Fullerene, VNF and their complexes were designed by Nanotube modeler 1.3.0.3 and GuassView 6 softwares [20, 21]. At the first step, the designed structures were optimized geometrically. Then, IR, NBO and FMO computations were implemented on

them. All of the computations were performed by Gaussian 16 software [22] by the density functional theory method in the B3LYP/6-31G (d) level of theory because in former studies about nanomaterials its results were in a good agreement with the experimental data. All of the calculations were implemented in the vacuum and in the temperature range of 298-398 at 10˚ intervals.

The studied processes were as follows:

VNF + Fullerene ⟶ NTP-Fullerene (1)

The values of adsorption energy values (E_{ad}) and thermodynamic parameters including adsorption enthalpy changes (ΔH_{ad}), Gibbs free energy changes (ΔG_{ad}), entropy changes (ΔS_{ad}), and thermodynamic equilibrium constants (K_{th}) were calculated by Equations 2-6 respectively.

$$E_{ad} = \left(E_{(\text{VNF-Fullerene})} - \left(E_{(\text{VNF})} + E_{(\text{Fullerene})} + E_{(\text{BSSE})}\right)\right) \quad (2)$$

$$\Delta H_{ad} = \left(H_{(\text{VNF-Fullerene})} - \left(H_{(\text{VNF})} + H_{(\text{Fullerene})}\right)\right) \quad (3)$$

$$\Delta G_{ad} = \left(G_{(\text{VNF-Fullerene})} - \left(G_{(\text{VNF})} + G_{(\text{Fullerene})}\right)\right) \quad (4)$$

$$\Delta S_{ad} = \left(S_{(\text{VNF-Fullerene})} - \left(S_{(\text{VNF})} + S_{(\text{Fullerene})}\right)\right) \quad (5)$$

$$K_{th} = \exp\left(-\frac{\Delta G_{ad}}{RT}\right) \quad (6)$$

In the referred equations, E is the total electronic energy of each structure, E_{BSSE} denotes the basis set superposition correction energy, H stands for enthalpy of the evaluated materials. The G denotes Gibbs free energy, S is the thermal correction of entropy, R is the ideal gas constants, T denotes the temperature [9-11].

Equations 7–12 were used to calculate the bandgap (E_g), chemical hardness (η), chemical potential (μ), maximum charge capacity (ΔN_{max}), and the electrophilicity (ω) of frontier molecular orbitals [32].

$$E_g = E_{LUMO} - E_{HOMO} \quad (7)$$

$$\%\Delta E_g = \frac{E_{g2} - E_{g1}}{Eg1} \times 100 \quad (8)$$

$$\eta = {(E_{LUMO} - E_{HOMO})}/{2} \quad (9)$$

$$\mu = {(E_{LUMO} + E_{HOMO})}/{2} \quad (10)$$

$$\omega = {\mu^2}/{2\eta} \quad (11)$$

$$\Delta N_{max} = -{\mu}/{\eta} \quad (12)$$

E_{LUMO} and E_{HOMO} in equation 6 are the energy of the lowest unoccupied molecular orbital and the energy

of the highest occupied molecular orbital respectively. The E_{g1} and E_{g2} in Equation 7, are the bandgap of NTP-C_{20} complex and bandgap of C_{20} respectively [12-14].

4. Conclusion

VNF is an antidepressant medication that is prescribed for the treatment of depression and anxiety disorders. This medicine has serious adverse side effects in high dosages and even can be lethal in the case of overdose. Therefore, VNF determination is very important. In this research, the performance of C_{20} as a novel sensing material for the construction of new electrochemical sensors to VNF measurement was evaluated by DFT computations. The values of adsorption energy and thermodynamic parameters showed VNF interaction with fullerene is exothermic, spontaneous and experimentally possible. The tangible increase of bandgap of fullerene in the adsorption process showed this nanostructure is a suitable sensing material for the electrochemical detection of VNF.

References

[1] M. A. Khalilzadeh, S. Tajik, H. Beitollahi, and R. A. Venditti. Green synthesis of magnetic nanocomposite with iron oxide deposited on cellulose nanocrystals with copper (Fe3O4@ CNC/Cu): investigation of catalytic activity for the development of a venlafaxine electrochemical sensor. *Ind. Eng. Chem. Res.*59 (2020) 4219-4228.

[2] M. P. Jahani, H. Akbari Javar, and H. Mahmoudi-Moghaddam. A new electrochemical sensor based on Europium-doped NiO nanocomposite for detection of venlafaxine. *Measurement* 173 (2021) 108616.

[3] S. Tajik, H. Beitollahi, Z. Dourandish, K. Zhang, Q. Van Le, T. Phan Nguyen, S. Young Kim, and M. Shokouhimehr. Recent advances in the electrochemical sensing of venlafaxine: an antidepressant drug and environmental contaminant. *Sensors* 20 (2020) 3675.

[4] H. Beitollahi, F. Garkani Nejad, S. Tajik, S. Jahani, P. Biparva, Voltammetric determination of amitriptyline based on graphite screen printed electrode modified with a Copper Oxide nanoparticles, Int. J. Nano. Dimens., 8 (2017) 197-205.

[5] T. Madrakian, R. Haryani, M. Ahmadi, and A. Afkhami. A sensitive electrochemical sensor for rapid and selective determination of venlafaxine in biological fluids using carbon paste electrode modified with molecularly imprinted polymer-coated magnetite nanoparticles. J. *Iran. Chem. Soc.* 13 (2016) 243-251.

[6] R. Zaimbashi, A. Mostafavi, T. Shamspur. ZnO nanoflower based electrochemical sensor for the selective determination of venlafaxine. J. *Iran. Chem. Soc.* 22 (2021) 1-9.

[7] C. K. Markopoulou, E. T. Malliou, J. E. Koundourellis, Application of two chemometric methods for the determination of imipramine, amitriptyline and perphenazine in content uniformity and drug dissolution studies. J. Pharm. Biomed. Anal., 37 (2005) 249–258.

[8] Q. Lanting, S. Durairaj, S. Prins, and A. Chen. Nanomaterial-based electrochemical sensors and biosensors for the detection of pharmaceutical compounds. *Biosens. Bioelectron.* 175 (2021) 112836.

[9] M. R. Jalali Sarvestani, R. Ahmadi, Investigating the Effect of Fullerene (C20) Substitution on the Structural and Energetic Properties of Tetryl by Density Functional

Theory. J. Phys. Theor. Chem. IAU. Iran., 15 (2018) 15-25.
[10] R. Ahmadi, M. R. Jalali Sarvestani, Adsorption of Tetranitrocarbazole on the Surface of Six Carbon-Based Nanostructures: A Density Functional Theory Investigation. Phys. Chem. B., 14 (2020) 198-208.
[11] M. R. Jalali Sarvestani, R. Ahmadi, Adsorption of TNT on the surface of pristine and N-doped carbon nanocone: A theoretical study. Asian J. Nanosci. Mater., 3 (2020) 103-114.
[12] M. R. Jalali Sarvestani, M. Gholizadeh Arashti, B. Mohasseb, Quetiapine Adsorption on the Surface of Boron Nitride Nanocage (B12N12): A Computational Study. Int. J. New. Chem., 7 (2020) 87-100.
[13] M. R. Jalali Sarvestani, R. Ahmadi, Investigating the Complexation of a recently synthesized phenothiazine with Different Metals by Density Functional Theory. Int. J. New. Chem., 4 (2017) 101-110.
[14] M. R. Jalali Sarvestani, R. Ahmadi, Adsorption of Tetryl on the Surface of B12N12: A Comprehensive DFT Study. Chem. Methodol., 4 (2020) 40-54.
[15] S. Majedi, F. Behmagham, M. Vakili, Theoretical view on interaction between boron nitride nanostructures and some drugs. J. Chem. Lett., 1 (2020) 19-24.
[16] H. G. Rauf, S. Majedi, E. A. Mahmood, M. Sofi, Adsorption behavior of the Al- and Ga-doped B12N12 nanocages on COn (n=1, 2) and HnX (n=2, 3 and X=O, N): A comparative study. Chem. Rev. Lett., 2 (2019) 140-150.
[17] R. A. Mohamed, U. Adamu, U. Sani, S. A. Gideon, A. Yakub, Thermodynamics and kinetics of 1-fluoro-2-methoxypropane vs Bromine monoxide radical (BrO): A computational view. Chem. Rev. Lett., 2 (2019) 107-117.
[18] S. Majedi, H. G. Rauf, M. Boustanbakhsh, DFT study on sensing possibility of the pristine and Al- and Ga-embeded B12N12 nanostructures toward hydrazine and hydrogen peroxide and their analogues. Chem. Rev. Lett., 2 (2019) 176-186.
[19] R. Moladoust, Sensing performance of boron nitride nanosheets to a toxic gas cyanogen chloride: Computational exploring. Chem. Rev. Lett., 2 (2019) 151-156.
[20] Nanotube Modeler J. Crystal. Soft., 2014 software.
[21] GaussView, Version 6.1, R. Dennington, T. A. Keith, J. M. Millam, Semichem Inc., Shawnee Mission, KS, 2016.
[22] Gaussian 16, Revision C.01, M. J. Frisch, G. W. Trucks, H. B. Schlegel, G. E. Scuseria, M. A. Robb, J. R. Cheeseman, G. Scalmani, V. Barone, G. A. Petersson, H. Nakatsuji, X. Li, M. Caricato, A. V. Marenich, J. Bloino, B. G. Janesko, R. Gomperts, B. Mennucci, H. P. Hratchian, J. V. Ortiz, A. F. Izmaylov, J. L. Sonnenberg, D. Williams-Young, F. Ding, F. Lipparini, F. Egidi, J. Goings, B. Peng, A. Petrone, T. Henderson, D. Ranasinghe, V. G. Zakrzewski, J. Gao, N. Rega, G. Zheng, W. Liang, M. Hada, M. Ehara, K. Toyota, R. Fukuda, J. Hasegawa, M. Ishida, T. Nakajima, Y. Honda, O. Kitao, H. Nakai, T. Vreven, K. Throssell, J. A. Montgomery, Jr., J. E. Peralta, F. Ogliaro, M. J. Bearpark, J. J. Heyd, E. N. Brothers, K. N. Kudin, V. N. Staroverov, T. A. Keith, R. Kobayashi, J. Normand, K. Raghavachari, A. P. Rendell, J. C. Burant, S. S. Iyengar, J. Tomasi, M. Cossi, J. M. Millam, M. Klene, C. Adamo, R. Cammi, J. W. Ochterski, R. L. Martin, K. Morokuma, O. Farkas, J. B. Foresman, and D. J. Fox, Gaussian, Inc., Wallingford CT, 2016.
[23] N. M. O'Boyle, A. L. Tenderholt, K. M. Langner, A Library for Package-Independent Computational Chemistry Algorithms. J. Comp. Chem., 29 (2008) 839-845.